

Angular Analysis of $B \rightarrow K^* \ell^+ \ell^-$ in *BABAR*

Jack L. Ritchie
Department of Physics
University of Texas at Austin
Austin, TX 78712, USA
Representing the BABAR Collaboration

Proceedings of CKM 2012, the 7th International Workshop on the CKM Unitarity Triangle, University of Cincinnati, USA, 28 September - 2 October 2012

1 Introduction

Flavor-changing neutral current B meson decays based on the process $b \rightarrow s \ell^+ \ell^-$ (where $\ell = e$ or μ), such as $B \rightarrow K^* \ell^+ \ell^-$, provide promising probes for new physics. The decays proceed through loop diagrams such as those shown in Figure 1.

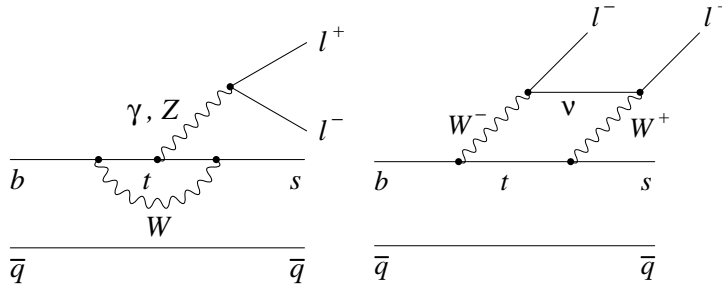


Figure 1: The electroweak penguin (left) and W -box (right) diagrams responsible for $B \rightarrow K^{(*)} \ell^+ \ell^-$ decays.

The theoretical treatment of $b \rightarrow s \ell^+ \ell^-$ transitions in the Standard Model (SM) follows an effective field theory approach in which the Hamiltonian is a sum of terms consisting CKM factors and Wilson coefficients that multiply operators formed from the light quark and lepton fields. The Wilson coefficients, obtained by integrating out the heavy particles, characterize the short-distance physics in these decays. New physics would modify the Wilson coefficients by providing new particles inside the loops and may modify the Hamiltonian by adding additional scalar or pseudoscalar terms. To account for QCD effects that mix the operators, so-called effective Wilson coefficients are defined. Measurements of $b \rightarrow s \ell^+ \ell^-$ decays probe the effective Wilson

coefficients C_7^{eff} , C_9^{eff} , and C_{10}^{eff} .¹ However, branching fraction measurements alone are not sufficient to exploit this opportunity, since they are generally in good agreement with SM theory predictions, even when measured versus q^2 ($= m_{\ell\ell}^2$) as shown in Figure 2.

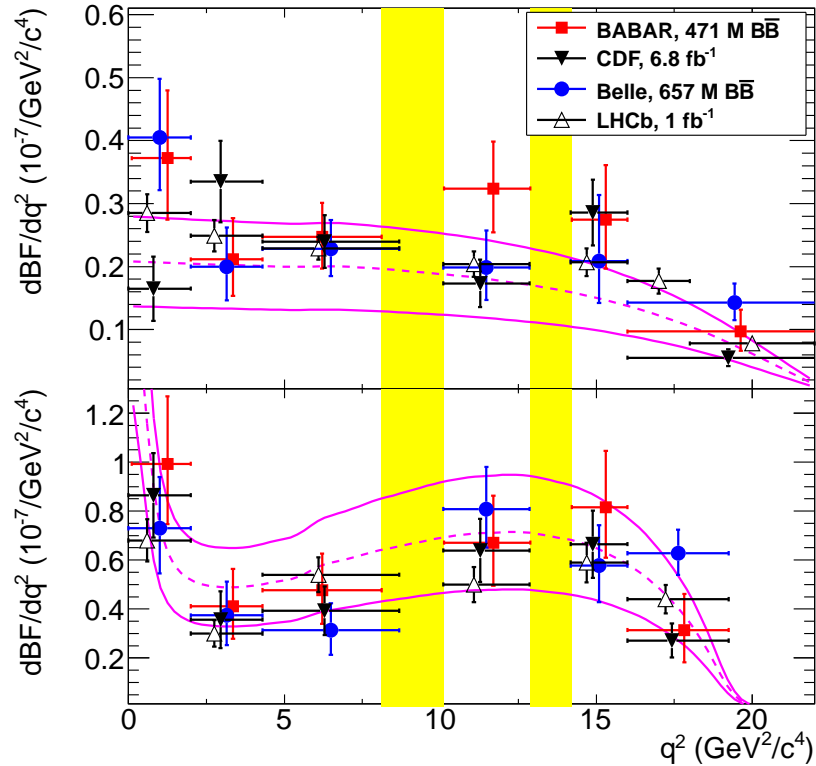


Figure 2: Partial branching fractions versus q^2 for $B \rightarrow K\ell^+\ell^-$ (top) and $B \rightarrow K^*\ell^+\ell^-$ (bottom) for BABAR[1], Belle[2], CDF[3], and LHCb[4, 5]. CDF and LHCb results are for $\mu^+\mu^-$ modes only. The region between the magenta curves shows the SM range.[6] Yellow shading shows the charmonium exclusion region used by BABAR.

More incisive observables are needed. Of particular interest is the lepton forward-backward asymmetry, A_{FB} , which in the SM exhibits a predictable q^2 dependence that includes a zero-crossing point near $q^2 = 4 \text{ GeV}^2/c^4$. Non-SM processes may change the magnitudes and relative signs of the relevant Wilson coefficients, and induce relative complex phases between them, and in general may lead to large deviations of A_{FB} versus q^2 from its SM expectation.

¹ C_7^{eff} represents the electromagnetic penguin; its magnitude is also probed by $b \rightarrow s\gamma$. C_9^{eff} and C_{10}^{eff} represent vector and axial-vector components, respectively, of the Z-penguin and W-box diagrams.

In this note, *BABAR*'s final (but still preliminary) angular analysis of the $B \rightarrow K^*\ell^+\ell^-$ decays is presented, based on a sample of 465 million $B\bar{B}$ pairs collected at the $\Upsilon(4S)$ at the SLAC PEP-II B-factory. This includes measurements of F_L , the fraction of longitudinal K^* polarization, and lepton forward-backward asymmetry A_{FB} in six q^2 bins (as defined in Table 1).

2 Data Analysis

In this analysis $B \rightarrow K\ell^+\ell^-$ and $B \rightarrow K^*\ell^+\ell^-$ events are reconstructed in nine distinct submodes: $B^+ \rightarrow K^+e^+e^-$, $B^+ \rightarrow K^+\mu^+\mu^-$, $B^0 \rightarrow K_S^0e^+e^-$, $B^0 \rightarrow K_S^0\mu^+\mu^-$; $B^+ \rightarrow K^+\pi^0e^+e^-$, $B^+ \rightarrow K_S^0\pi^+e^+e^-$, $B^+ \rightarrow K_S^0\pi^+\mu^+\mu^-$, $B^0 \rightarrow K^+\pi^-e^+e^-$, and $B^0 \rightarrow K^+\pi^-\mu^+\mu^-$, with $K_S^0 \rightarrow \pi^+\pi^-$. Charge conjugation is implied here and throughout this note. The submode $B^+ \rightarrow K^+\pi^0\mu^+\mu^-$ is excluded from this analysis since Monte Carlo simulations indicated that it did not improve the results. Events where the dilepton pair originated from J/ψ or $\psi(2S)$ decays are explicitly removed using selection criteria applied to $m_{\ell\ell}$. The major background sources are semi-leptonic B and D decays, which are suppressed by applying optimized cuts on bagged decision tree outputs. The bagged decision trees utilize event shape variables, vertex information, missing energy, and similar inputs to discriminate between signal and background events. Training is carried out on Monte Carlo samples. An additional background from $B^+ \rightarrow D\pi^+$, followed by $D \rightarrow K^*\pi$ along with $\pi \rightarrow \mu$ misidentification, is vetoed explicitly by rejecting $K^*\pi$ combinations near the D mass. After all selection criteria have been applied, the signal efficiency is typically about 15%, although it varies by submode and q^2 -bin.

After event selection, a sequence of three maximum likelihood fits is performed to determine signal yields in each q^2 -bin and to determine F_L and A_{FB} . The first fit determines the number of signal events in each q^2 -bin. It is performed in three dimensions: m_{ES} , $M(K\pi)$, and \mathcal{L} , where $m_{ES} = \sqrt{E_{\text{beam}}^*{}^2 - p_B^*{}^2}$, $M(K\pi)$ is the mass of the K^* candidate, and \mathcal{L} is a likelihood ratio formed from the output of the bagged decision trees used to separate signal events from other B meson decays. E_{beam}^* and p_B^* are the beam energy and momentum of the B in the $\Upsilon(4S)$ frame (CM).

The subsequent fits are performed for the signal enriched region defined by $m_{ES} > 5.27$ GeV. In the second fit, a fourth dimension is added, $\cos\theta_K$, where θ_K is the angle between the K and the B in the K^* rest frame. The yields determined from the first fit are fixed in the second fit, and the parameter F_L is determined based on the equation:

$$\frac{1}{\Gamma} \frac{d\Gamma}{d\cos\theta_K} = \frac{3}{2}F_L \cos^2\theta_K + \frac{3}{4}(1 - F_L)(1 - \cos^2\theta_K) \quad (1)$$

In the final fit, F_L is fixed at the result of the previous fit, and a fifth dimension is added, $\cos\theta_\ell$, where θ_ℓ is the angle between the ℓ^+ (ℓ^-) and the B (\bar{B}) in the dilepton

rest frame. The parameter A_{FB} is determined from the fit based on the equation:

$$\frac{1}{\Gamma} \frac{d\Gamma}{d \cos \theta_\ell} = \frac{3}{4} F_L (1 - \cos^2 \theta_\ell) + \frac{3}{8} (1 - F_L) (1 + \cos^2 \theta_\ell) + A_{FB} \cos \theta_\ell \quad (2)$$

The fit methodology was validated using both Monte Carlo test experiments and by fits to $B \rightarrow K^* J/\psi$ and $B \rightarrow K^* \psi(2S)$ modes in data for which prior measurements exist.

3 Results

Preliminary *BABAR* results for F_L and A_{FB} versus q^2 are given in Table 1. While the dominant errors are statistical, systematic error estimates are included in Table 1. Figure 3 shows these results along with results reported thus far by other experiments.

q^2 bin (GeV ² /c ⁴)	F_L	A_{FB}
0.1 - 2.0	$0.23_{-0.09}^{+0.10} \pm 0.04$	$0.14_{-0.16}^{+0.15} \pm 0.20$
2.0 - 4.3	$0.15_{-0.14}^{+0.17} \pm 0.04$	$0.40_{-0.22}^{+0.18} \pm 0.07$
4.3 - 8.1	$0.32 \pm 0.12 \pm 0.06$	$0.15 \pm 0.16 \pm 0.08$
10.1 - 12.9	$0.40 \pm 0.12 \pm 0.06$	$0.36_{-0.17}^{+0.16} \pm 0.10$
14.2 - 16.00	$0.43_{-0.13}^{+0.10} \pm 0.09$	$0.34_{-0.15}^{+0.08} \pm 0.07$
> 16.00	$0.55_{-0.17}^{+0.15} \pm 0.03$	$0.34_{-0.21}^{+0.19} \pm 0.07$
1.00 - 6.00	$0.25_{-0.08}^{+0.09} \pm 0.03$	$0.17_{-0.14}^{+0.12} \pm 0.07$

Table 1: Preliminary *BABAR* results for F_L and A_{FB} versus q^2 . In addition F_L and A_{FB} measurements are provided in a bin (1.00 - 6.00) that is sometimes used by theorists. The first error is statistical and the second is systematic.

4 Conclusions

Significant progress has been made in the study of $b \rightarrow s \ell^+ \ell^-$ related B decays. Thus far no significant deviations from the SM have been observed. Figure 3 shows that the current results from all experiments are generally consistent with each other and with the SM expectations for F_L and A_{FB} . However, for meaningful comparisons of these angular measurements with theory, much larger data sets are needed. LHCb measurements will improve as additional data is collected. Future super-B factory results will also be important since a larger number of final states will be accessible.

This work was supported in part by Department of Energy contract DE-AC02-76SF00515.

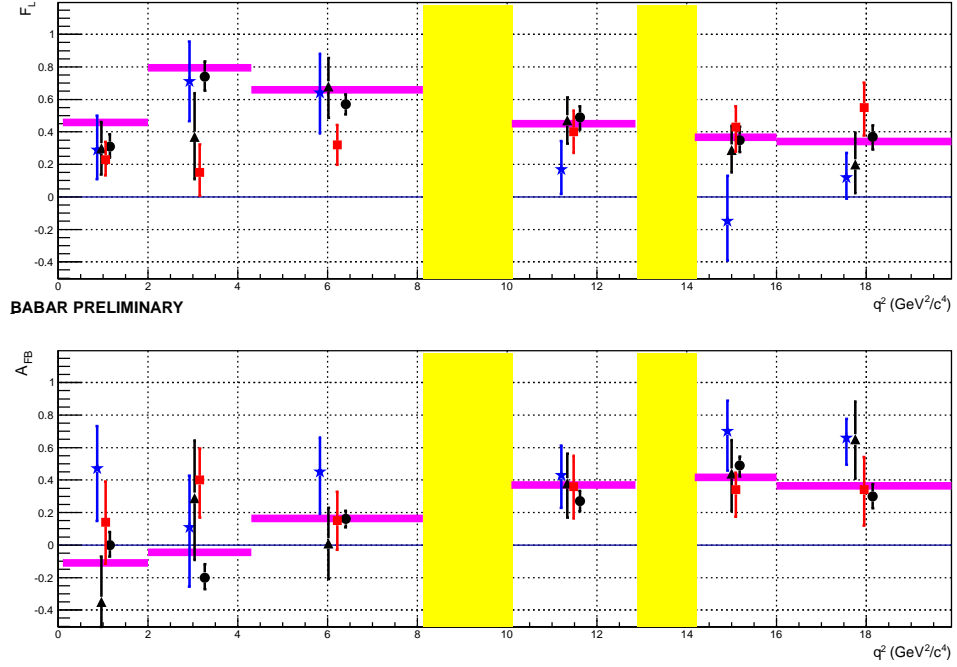


Figure 3: Results for F_L (top) and A_{FB} (bottom) versus q^2 . *BABAR* preliminary results are indicated by the solid red squares. Results from other experiments are: Belle[2] blue stars, CDF[7] black triangles, and LHCb[5] solid black dots. Yellow shading indicates the charmonium exclusion region. The binned SM theory prediction [8] is shown in magenta.

References

- [1] J. L. Lees *et al.* [*BABAR* Collaboration], Phys. Rev. D **86**, 032012 (2012).
- [2] J.-T. Wei *et al.* [*Belle* Collaboration], Phys. Rev. Lett. **103**, 171801 (2009).
- [3] T. Aaltonen *et al.* [*CDF* Collaboration], Phys. Rev. Lett. **107**, 201802 (2012).
- [4] R. Aaij *et al.* [*LHCb* Collaboration], LHCb-PAPER-2012-024, arXiv:1209.4284.
- [5] LHCb Collaboration, LHCb-CONF-2012-008.
- [6] A. Ali *et al.*, Phys. Rev. D **66**, 034002 (2002).
- [7] T. Aaltonen *et al.* [*CDF* Collaboration], Phys. Rev. Lett. **108**, 081807 (2012).
- [8] A. Ali *et al.*, Phys. Rev. D **61** 074024 (2000); A. Ali *et al.*, Phys. Rev. D **66**, 034002 (2002); and Ball *et al.*, Phys. Rev. D **75**, 054004 (2007).